united nations
educational, scientific
and cultural
organization

international atomic
energy agency

the
abdus salam
international centre for theoretical physics

SMR: 1513/8

10TH CONFERENCE ON HOPPING AND RELATED PHENOMENA

(1 - 4 September 2003)

"Crossover from Weak Localization to Weak Anti-Localization with Decreasing Thickness of Sn-Doped InSb Films on GaAs (100) Substrates"

presented by:

S. ISHIDA

Tokyo University of Science
Yamaguchi
Japan

Crossover from Weak Localization to Weak Anti-Localization with Decreasing Thickness of Sn-Doped InSb Films on GaAs (100) Substrates

S. ISHIDA[1] (a), K. TAKEDA (a), A. OKAMOTO (b) and I. SHIBASAKI (b)

(a) *Faculty of Science & Engineering, Tokyo University of Science, Yamaguchi, Onoda,*
Yamaguchi 756-0884, JAPAN
(b) *Asahi Kasei Corporation, Samejima 2-1, Fuji, Shizuoka 416-8501, JAPAN*

Subject classification: 73.40.-c; 73.50.-h; S7.13

Magnetoresistance (MR) effects caused by quantum interference have been investigated in order to search into the spin-orbit interaction (SOI) in the InSb films grown on GaAs(100) substrates by MBE. The positive MR for the 0.1 μm thick undoped film with anisotropy between parallel and perpendicular field orientation arising from the 2D weak anti-localization (WAL) in the accumulation layer at the InSb/GaAs interface has been explained by taking account of the spin-Zeeman effect on the SOI caused by the asymmetric potential at the hetero interface (Rashba term); the zero-field spin splitting energy of Δ_0 ~ 13 meV with SO scattering rate τ_{so}^{-1} ~ 1.7 × 10^{12} s, the electron effective mass of m^* ~ $0.10m_0$ seven times of the band edge mass in bulk InSb and the effective g-factor of $|g^*|$ ~ 15 have been inferred from the fits of MR with the 2D WL theory. In Sn-doped films, the negative MR found in extremely weak magnetic fields far before the appearance of the Shubnikov-de Haas (SdH) oscillations dramatically crossovers to the positive MR with decreasing the film thickness from d = 1 μm to 0.1 μm. These results have been analyzed using a two-layer model for the films, where the composition of upper layer under the surface and lower one adjacent to the InSb/GaAs interface is assumed; the SO scattering rate in the intrinsic InSb film due to the bulk inversion asymmetry (Dresselhaus term) has been found to be as small as $\tau_{so}^{-1} \leq 10^9$ s^{-1} and when the interface is approached in the film the WL crossovers to the WAL with the increase of SOI in the layers caused by the increased influence of the Rashba electric field.

Introduction Among the narrow-gap III-V semiconductors, InSb has the highest mobility with the smallest electron effective mass (m^* ~ $0.014m_0$) and the largest negative effective g-factor ($|g^*|$ = 51 ~ 35 according to the carrier concentration n = 10^{14} ~ 10^{17}cm^{-3} [1, 2]). Its thin layers are often grown on semi-insulating GaAs substrates using molecular-beam epitaxy (MBE) for device applications such as magnetic-field sensors [3, 4] and high-speed devices [5]. However, a large lattice mismatch between InSb and GaAs induces high-density misfit dislocations at the InSb/GaAs interface, which results in an extraordinarily large carrier accumulation at the interface [6]. In undoped films, the carriers at the InSb/GaAs interface [7, 8] show the positive magnetoresistance (MR) with anisotropy between parallel and perpendicular orientation of magnetic field to the film, arising from the two-dimensional (2D) weak anti-localization (WAL) which reflects the interplay between the strong spin-orbit interaction (SOI) and spin-Zeeman effect. [9-11] In heavily Sn-doped InSb films with thickness $d \geq$ 0.5 μm, on the other hand, degenerated electrons in the films show the ordinary Shubnikov-de Haas (SdH) oscillations at low temperatures.

Two types of the SOI can be identified; one is the random SOI due to impurity potentials (Elliott mechanism) [12] and the other one arises from the spin splitting in asymmetric systems [Dyakonov-Perel (DP) mechanism]. The DP mechanism is affiliated with the crystal field arising from the lack of inversion symmetry in zinc-blende structures (Dresselhaus term) [13, 14] and the asymmetric potential in the hetero junction or quantum well (Rashba term) [16]. The latter is expected to be more significant in narrow-gap semiconductors [16-18] so that its dominance in the accumulation layer at the InSb/GaAs interface is expected.

In this paper, the MR effects caused by quantum interference have been investigated in order to search into the SOI in the InSb films on GaAs(100) substrates. The WAL in the accumulation layer has been studied for the undoped film 0.1 μm thick. The crossover from WL to WAL with decreasing the film thickness for Sn-doped films from d = 1 μm to 0.1 μm found in extremely weak magnetic fields far before the appearance of the SdH oscillations has been analyzed assuming a two-layer model

---

[1] Corresponding author; Tel/Fax: +81-836-4526; e-mail: ishida@ed.yama.tus.ac.jp

for the films; the WL crossovers to the WAL when the interface is approached in the film, with the increase of SOI in the layers caused by the increased influence of the Rashba electric field.

Experimental InSb thin films were grown directly on the semi-insulting GaAs(100) substrates, ignoring the large lattice mismatch between InSb and GaAs. The observation of transmission electron microscopy (TEM) shows the existence of a periodic distribution of misfit dislocations whose density is $N_{\mathrm{md}} \sim 1.3 \times 10^{13}$ cm^{-2} being consistent with the lattice mismatch of 14.6 %, since the misfit dislocations come from the correspondence of seven InSb(111) layers to eight GaAs(111) layers at the InSb/GaAs interface. The interface carrier density n_{i} is known to be proportional to N_{md} [6] despite that n_{i} is smaller than N_{md} in one order of magnitude. The films studied in this work are the nominally undoped one 0.1 μm thick and 7×10^{16} (7E16) cm^{-3} Sn doped ones with the thickness ranging d = 0.1 ~ 1.0 μm. These films were prepared under the same growth conditions except the film thickness for each doping level. The film parameters at 1.4 K are given in Table 1. The transverse and longitudinal magnetoresistance (MR) measurements have been carried out in both perpendicular and parallel magnetic fields to the film plane at 80 K and liquid He temperatures.

Results and Discussion In undoped films, the intrinsic carriers in a high-mobility InSb film have frozen-out at low temperatures and the low-mobility carriers in the accumulation layer at the InSb/GaAs interface dominates the low-temperature transport. [7, 8, 11] The effective thickness of the accumulation layer d_{a} is roughly estimated as ~ 20 nm from the magnetic field strength (~ 7.5 T) where the in-plane transverse MR with classical quadratic dependence starts to appear when $2l_{\mathrm{B}} = 2(\hbar/eB)^{1/2} = d_{\mathrm{a}}$ [l_{B}: magnetic length]. [19] The low-temperature MR for the undoped film shows a steep rise in weak magnetic fields with anisotropy between parallel- and perpendicular-field orientations as shown in Fig. 1(a). These MR data can be explained by the 2D WL theory taking account of the effect of Zeeman splitting on SO scattering, proposed by Maekawa and Fukuyama: [9,10]

$$\frac{\Delta R}{R_0} = -\frac{e^2 R_\square}{2\pi^2\hbar}\left\{ \ln\left(\frac{\tau_0}{\tau_1} + \frac{D\tau_0 t^2}{3l_{\mathrm{B}}^4}\right) - \frac{1}{2\sqrt{1-\gamma}}\left[\ln\left(\frac{\tau_0}{\tau_+} + \frac{D\tau_0 t^2}{3l_{\mathrm{B}}^4}\right) - \ln\left(\frac{\tau_0}{\tau_-} + \frac{D\tau_0 t^2}{3l_{\mathrm{B}}^4}\right)\right] - \ln\left(\frac{\tau_0}{\tau_1}\right)\right\} \quad (1)$$

for parallel magnetic fields (t: channel thickness) and

$$\frac{\Delta R}{R_0} = \frac{e^2 R_\square}{2\pi^2\hbar}\left\{ \psi\left(\frac{\tau_{\mathrm{B}}}{\tau_0} + \frac{1}{2}\right) - \psi\left(\frac{\tau_{\mathrm{B}}}{\tau_1} + \frac{1}{2}\right) - \frac{1}{2\sqrt{1-\gamma}}\left[\psi\left(\frac{\tau_{\mathrm{B}}}{\tau_+} + \frac{1}{2}\right) - \psi\left(\frac{\tau_{\mathrm{B}}}{\tau_-} + \frac{1}{2}\right)\right] - \ln\left(\frac{\tau_0}{\tau_1}\right)\right\} \quad (2)$$

for perpendicular fields, where

$$\tau_1^{-1} = \tau_\epsilon^{-1} + 2\tau_{\mathrm{s}}^{-1} + 4\tau_{\mathrm{so}}^{-1},$$

$$\tau_\pm^{-1} = \tau_\epsilon^{-1} + 6\tau_{\mathrm{s}}^{-1} + 2(\tau_{\mathrm{so}}^{-1} - \tau_{\mathrm{s}}^{-1})(1 \pm \sqrt{1-\gamma}),$$

$$\gamma = \left(\frac{g\mu_{\mathrm{B}} B}{2\hbar(\tau_{\mathrm{s}}^{-1} - \tau_{\mathrm{so}}^{-1})}\right)^2, \tau_{\mathrm{B}} = \frac{l_{\mathrm{B}}^2}{4D}, \; l_{\mathrm{B}} = \sqrt{\frac{\hbar}{eB}}$$

and $D = v_{\mathrm{F}}^2\tau_0/2$ (v_{F}: Fermi velocity) is the diffusion constant in 2D and μ_{B} the Bohr magneton. τ_0, τ_ϵ, τ_{so} and τ_{s} is the elastic, inelastic, SO and spin scattering times, respectively. The relevance of Zeeman splitting term in controlling WAL effects was studied experimentally using eqs. (1) and (2) by Kowal et al. for a Au-doped $\mathrm{In_2O_{3-x}}$ film. [20] Both perpendicular and parallel MR data for the undoped InSb film 0.1 μm thick have been fitted with the above equations. The best fits have been obtained for each orientation of magnetic field, as shown in Fig. 1. The effective g-value is inferred as $|g^*| \sim 15$ and the electron effective mass of $m^* \sim 0.10m_0$ seven times of the band edge mass in bulk InSb is determined from the mobility data with $\tau_0 \sim 1.8 \times 10^{-14}$ s, where $|g^*|$ and τ_0 are the fitting parameters used. In particular, the perpendicular and parallel MR data are consistent about the best-fit parameters except the inelastic scattering time τ_ϵ. The result has revealed the strong SOI ($\tau_{\mathrm{so}} \sim 5.8 \times 10^{-13}$ s) and the relevance of the spin-Zeeman effect to the WAL effect as well as weak spin scattering ($\Box_s \sim 1 \Box 10^{-10}$ s). Though the temperature dependence of $\Box_\Box$ shown in the inset of Fig. 1 seems to reflect the electron-electron interaction for a 2D system ($\Box_\Box$ μ T^{-x}), the value of x cannot be identified. Because the relation $\Box_\Box \gg \Box_0$ survives even up to ~ 100 K, a very wide range of temperature below about 100 K is found to be a WL regime. The inelastic scattering length $l_\Box = (D\Box_\Box)^{1/2}$ and the SO scattering one $l_{so} = (D\Box_{so})^{1/2}$ at 4.2K are ~ 50 nm and ~ 30 nm, respectively ($d_a < l_{so} < l_\Box$). The WL effect on the MR manifests itself more pronounced when $k_F l_e > 1$ where k_F is the Fermi wave number and $B < B_{tr} = \hbar/2el_e^2$ (transport magnetic field) for perpendicular field because it assumes the diffusion process where $l_B > 2^{1/2} l_e$. We obtain $k_F l_e \sim 2.1$ and $B_{tr} \sim 6.7$ T for the accumulation layer studied, assuming the 2D density of states $g = m^*/\Box\hbar^2$.

Through the above analysis of MR, the orbital and spin-Zeeman effects in electron-electron interaction (EEI) have been ignored. The characteristic field strengths to observe these effects on MR are $B_o \sim \Box kT/eD$ for the orbital effect and $B_s \sim 4\Box kT/|g^*|\,\Box_B$ for the spin effect [10, 21] where $D \sim 1.3 \Box 10^{-2}$ m^2/s and $|g^*| \sim 15$ ($B_o \sim 400$ G and $B_s \sim 2.5$ T at 2 K). The contribution from the orbital effect is small at low temperatures [22] and the magnetic field is not large enough for the development of the spin effect in EEI.

Sn-doped films with $d \geq 0.5$ □m show the clear SdH oscillations corresponding to the high Landau quantum numbers (N $\geq$ 4) below 1.5 T at low temperatures, but clear oscillations are not observed for $d = 0.3$ □m. Conspicuous MR effects rapidly growing with decreasing temperature with anisotropy between parallel and perpendicular magnetic fields have been found far before the appearance of the SdH oscillations. Fig. 2 shows the SdH oscillations observed in the transverse and longitudinal MR for $d = 1.0$ □m under in-plane magnetic fields at 1.4 K. The periods in B^{-1} plot of the oscillations are consistent with the carrier concentration obtained from Hall data. The negative MR observed in weak magnetic fields before the appearance of oscillations can be broadly divided into two regimes: T-sensitive one exhibiting a large peak at $B = 0$ below the critical field ($B_c \sim 30$ mT for parallel field) observed with anisotropy between parallel and perpendicular magnetic fields as seen in the inset of the figure and T-insensitive parabolic one due to the classical skipping orbit effect in the presence of specular surface scattering [23, 24] observable only in parallel magnetic fields with gradual dependence above B_c. The T-dependent negative MR below B_c can be further classified into two regimes: the WL effect indicating weak SOI in extremely weak magnetic fields ($B < B_x \sim 18$ mT for parallel field) and the negative MR exhibiting an abrupt dependence in higher fields ($B > B_x$).

The MR due to the WL effect in either orientation has been transfigured from the negative one with weak SOI into the positive one with decreasing the film thickness from $d = 1$ □m to 0.2 □m. Such features are shown in Fig. 3(a) for parallel fields and in Fig. 3(b) for perpendicular fields, as the change of transverse MC per sheet $\Box\Box_\Box(B) = \Box R/R_0R_\Box(B)$ in extremely weak magnetic fields for four films in the range $d = 1.0 \sim 0.1$ □m. Here, $\Box_\Box(B) \sim \Box_{xx}$ since $\Box B \ll 1$ in the range of magnetic field concerned depending on each film. These results have been analyzed for both parallel and perpendicular MC using a two-layer model in which the composition of upper layer under the surface and lower one adjacent to the InSb/GaAs interface of the film yielding parallel conduction channels is assumed; the sheet conductance for each decomposed layer has been inferred as $\Box(0.5\sim0.3) = \Box(0.5) - \Box(0.3)$, for example, where $\Box(0.5\sim0.3)$ means the sheet conductance $\Box_\Box$ for the upper part 0.2 □m thick of the film with $d = 0.5$ □m and $\Box(0.5)$ for the entire film 0.5 □m thick. The inelastic diffusion length $l_\Box$ is roughly estimated to be larger than 4, 4, 1 and 0.6 □m for the decomposed layer d(1.0~0.5), d(0.5~0.3), d(0.3~0.2) and d(0.2~0.1), respectively, so that $l_\Box > t$ for each layer. Since we obtain $B_{tr} \sim$ 3.2, 11.5, 45.8 and 218 mT for d = 1.0, 0.5, 0.3 and 0.2 □m, respectively, the value of B_{tr} for the layer d(1.0~0.5), d(0.5~0.3), d(0.3~0.2) and d(0.2~0.1) must be smaller than 3, 12, 46 and 220 mT, respectively. Moreover, we find that the characteristic field B_x dividing the WL effect from the abrupt decrease of the resistance observed for $d \geq 0.5$ □m in perpendicular fields agrees with B_{tr}; for example B_{tr} in perpendicular field is indicated in the inset of Fig. 2 for $d = 1$ □m. This means that the sharp negative MR above B_x (~ B_{tr}) probably relates to the WL effect [25] beyond the diffusive approximation. Thus, both parallel and perpendicular MC, $\Delta\sigma_{\square}(B)$, for each layer can be compared with eqs. (1) and (2), respectively, in the extremely weak magnetic fields.

Fig. 4(a) and (b) show the variations in parallel and perpendicular MC for the layers, respectively, where the best fits obtained are depicted. In the fitting routine, the value of $|g^*| \sim 37$ for bulk n-InSb with the same carrier concentration ($n \sim 7 \times 10^{16}$ cm^{-3}) [2] was used. The values of τ_{so} inferred from the fits of parallel and perpendicular MC for the decomposed layers are listed in Table 2, being consistent with each other in different orientation of magnetic field. One can see that τ_{so} of the layer decreases abruptly with approaching the interface from the distance of ~ 0.5 μm. From the above result, the variation of MC in the extremely weak magnetic fields for each decomposed layer has been explained as the crossover from the 2D WL to WAL with the increase of SOI in the layers: from the SO rate $\tau_{so}^{-1} \sim 1 \times 10^9$ s^{-1} in d(1.0~0.5) to 1.5×10^{11} s^{-1} in d(0.2~0.1) with approaching the InSb/GaAs interface, being caused by the increased influence of the asymmetric potential at the hetero interface (Rashba term). [15]

In the WL theory, we assume the Dyakonov-Perel (DP) mechanism for the SO scattering, where τ_{so} relates to the zero-field spin-splitting energy Δ_0 as $\tau_{so}^{-1} = <\Delta_0^2>\tau/4\hbar^2$. [14, 16, 17] For the accumulation layer at the InSb/GaAs interface, we infer $\Delta_0 \sim 13$ meV from $\tau_{so} = 5.8 \times 10^{-13}$ s obtained from the fits. This value is compared with $\Delta_0 \sim 5$ meV ($\tau_{so} \sim 7 \times 10^{-13}$ s) estimated for the 2D electron gas in the inversion layer at the InSb/CdTe hetero junction by Greene et al. [26, 27] In bulk n-InSb, there has so far been no observation of the WAL effect. The negative MR due to WL was observed by Mani et al. in a lightly doped n-InSb ($n = 5 \times 10^{14}$ cm^{-3}) [28], where the WL correction was recognized in weak magnetic fields up to $B \sim 30$ mT and the data were fitted to the 3D WL theory [29] with $\tau_{so}^{-1} \sim 0$. Probably, our result of $\tau_{so}^{-1} \sim 1 \times 10^9$ s^{-1} for the bulk-like decomposed layer d(1.0~0.5) barely measures the SOI induced by bulk inversion asymmetry (Dresselhaus term) [13, 14] in the intrinsic InSb film.

In conclusion, our result on the variation of the SO rate in the growth direction of InSb film deduced with the aid of a simple two-layer model has revealed that the SO rate in the intrinsic InSb film due to the bulk crystal field is as small as $\tau_{so}^{-1} \leq 10^9$ s^{-1} and the asymmetric potential at the InSb/GaAs(100) interface strongly affects the InSb layer inside the range up to ~ 0.5 μm from the interface.

Refernces

[1] R. A. ISAACSON, Phys. Rev. **169**, 312 (1968).
[2] N. G. GLUZMAN, L. D. SABIRZAYANOVA and I. TSIDIL'KOVSKII, Sov. Phys.Semicond. **13**, 275 (1979).
[3] J. HEREMANS, D. L. PARTIN, C. M. THRUSH and L. GREEN, Semicond. Sci. Technol. **8** , 424 (1993).
[4] I. SHIBASAKI, J. Cryst. Growth **175/176**, 13 (1997).
[5] T. ASHLEY, A. B. DEAN, C. T. ELLIOT, G. J. PRYCE, A.D. JOHNSON and H. WILLIS, Appl. Phys. Lett. **66**, 481 (1995).
[6] T. TANAKA, M. WASHIMA and H. SAKAGUCHI, Jpn. J. Appl. Phys. **38**, 1107 (1999).
[7] S. N. SONG, J. B. KETTERSON, Y. H. CHOI, R. SUDHARSANON and M. RAZEGHI, Appl. Phys. Lett. **63**, 964 (1993).
[8] J. HEREMANS, D. L. PARTIN, D. T. MORELLI, C. M. THRUSH, G. KARCZEWSKI and K. FURDYNA, J. Appl. Phys. Lett. **74**, 1793 (1993).
[9] S. MAEKAWA and H. FUKUYAMA, J. Phys. Soc. Jpn. **50**, 2131 (1981).
[10] See, e.g., S. KOBAYASHI and F. KOMORI, Progr. Theor. Phys. **84**, 224 (1985), and references therein.
[11] S. ISHIDA, K. TAKEDA, A. OKAMOTO and I. SHIBASAKI, Proc. Int. Conf. on Quantum Transport and Quantum Interference (Localisation 2002), J. Phys. Soc. Jpn. **72** Suppl. A, 153 (2003).
[12] R. J. ELLIOTT, Phys. Rev. **96**, 266 (1954).
[13] G. F. DRESSELHAUS, Phys. Rev. **100**, 580 (1955).
[14] P. D. DRESSELHAUS, C. M. M. PAPAVASSILIOU, R.G. WHEELER, R. N. SACKS, Phys. Rev. Lett. **68**, 106 (1992).
[15] Y. A. BYCHKOV and E. I. RASHBA, J. Phys. C **17**, 6039 (1984).
[16] D. L. CHEN, J. HAN, S. DATTA and D. B. JANES, Phys. Rev. B **47**, 4084 (1993).
[17] W. KNAP, C. SKIERBISZEWSKI, A. ZDUNIAK, E. LITWIN-STASZEWSKA, D. BERTHO, F. KOBBI, J. L. ROBERT, G. E. PIKUS F.G. PIKUS, S. V. IORDANSKII, V. MOSSER, K. ZEKENTES and Yu. B. LYANDA-GELLER,

Phys. Rev. B **53**, 3912 (1996).
[18] G. LOMMER, F. MALCHER and U. ROESSLER, Phys. Rev. Lett. **60**, 728 (1988).
[19] A. FUJIMOTO, H. KOBORI, T. OHYAMA, S. ISHIDA, K. SATO, T. KUSAKA, Y. KAKEHI, I. SHIBASAKI, Proc. 10th Int. Conf. on Narrow Gap Semiconductors, Ishikawa, Japan (2001) [IPAP Conference Series **2** (2001)] 236.
[20] D. KOWAL, M. BEN-CHORIN, Z. OVADTAHU, Phys. Rev. B **44**, 9080 (1991).
[21] S. MORITA, N. MIKOSHBA, Y. KOIKE, T. FUKASE, S. ISHIDA and M. KITAGAWA, Solid State Electronics **28** (1985) 113.
[22] S. KAWAJI, Progr. Theor. Phys. **84**, 178 (1985),
[23] K. K. CHOI, D. C. TSUI, S. C. PALMATEER, Phys. Rev. B **33**, 8216 (1986).
[24] R. P. TAYLOR, P. C. MAIN, L. EAVES, S. P. BEUMOBT, I. MCINTYRE, S. THOMAS, C. D. W. WILKINSON, J. Phys. Condens, Matter **1**, 10413 (1989).
[25] H. P. WITTMAN, A.SHMID, J. Low Temp. Phys. **69**, 131 (1987).
[26] S. K. GREENE, J. SINGLETON, T. D. GOLDING, M. PEPPER, C. J. G. M. LANGERAK, J. H. DINAN, Surf. Sci. **228** (1990) 542.
[27] S. LAMARI, J. Appl. Phys. **91** (2002) 1698.
[28] R. G. MANI, L. GHENIM, J. B. CHOI, Phys. Rev. B **43** (1991) 12630.
[29] A. KAWABATA, Solid State Commun. **34** (1973) 397.

Tables

Table 1. Film parameters at 1.4 K.

d (μm)	$n_{\square}$ (10^{12}cm^{-2})	$R_{\square}$ (Ω)	μ (10^4cm^2/Vs)	l_e (nm)	$k_F l_e$
0.10 (undoped)	1.44	12200	0.0356	7.0	2.1
0.11 (Sn doped)	0.84	7560	0.0978	8.7	1.2
0.21 (Sn doped)	1.16	1080	0.495	39	4.7
0.32 (Sn doped)	1.75	273	1.13	87	10
0.53 (Sn doped)	3.35	96.0	2.05	170	20
1.01 (Sn doped)	8.07	21.5	3.64	320	43

Table 2. SO scattering. time τ_{so} inferred from the fits of parallel and perpendicular MC for the decomposed layers.

	d (1.0~0.5)	d (0.5~0.3)	d (0.3~0.2)	d (0.2~0.1)
$\tau_{SO\,//}$ (ps)	560	200	42	7.5
$\tau_{SO\,\perp}$ (ps)	940	420	47	6.0

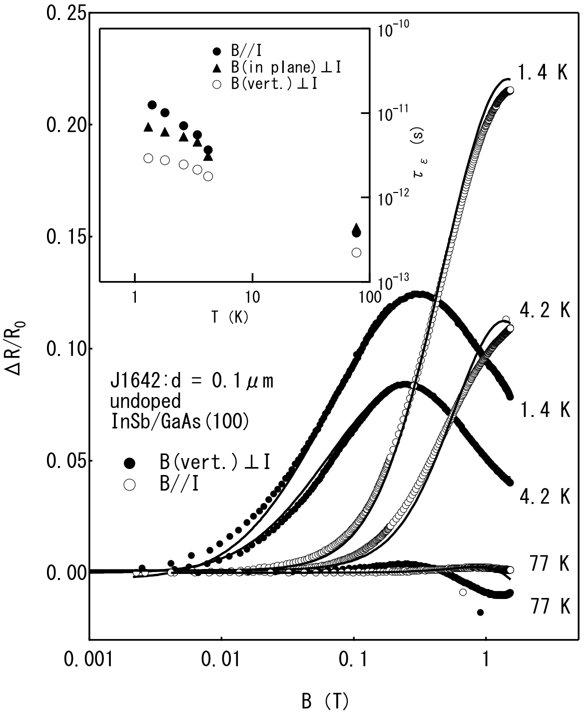

Fig. 1 Transverse magnetoresistance (MR) in perpendicular magnetic fields and longitudinal MR in parallel fields for the undoped film ($d = 0.1$ μm) at various temperatures. Solid lines are the results of fits. Inset: Temperature dependence of the inelastic scattering time τ_ε inferred from the fits for three orientations of applied magnetic field.

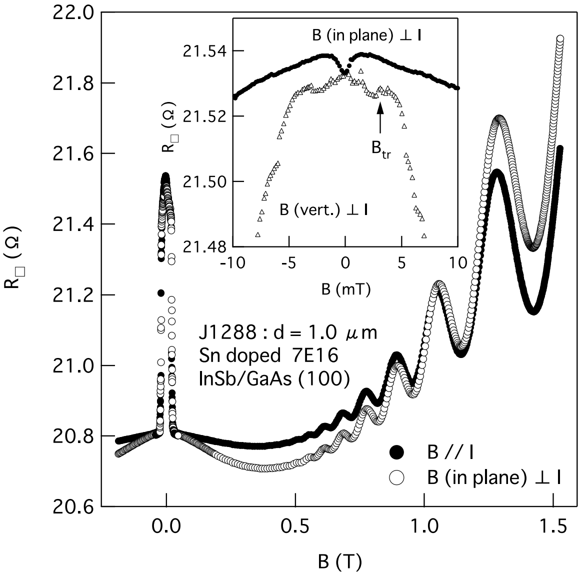

Fig. 2 SdH oscillations and anomalous negative MR in weak magnetic fields in the transverse and longitudinal MR under in-plane magnetic fields for Sn doped film 1 μm thick at 1.4 K. Inset: perpendicular and parallel MR in very weak magnetic fields, where B_{tr} for perpendicular field is indicated.

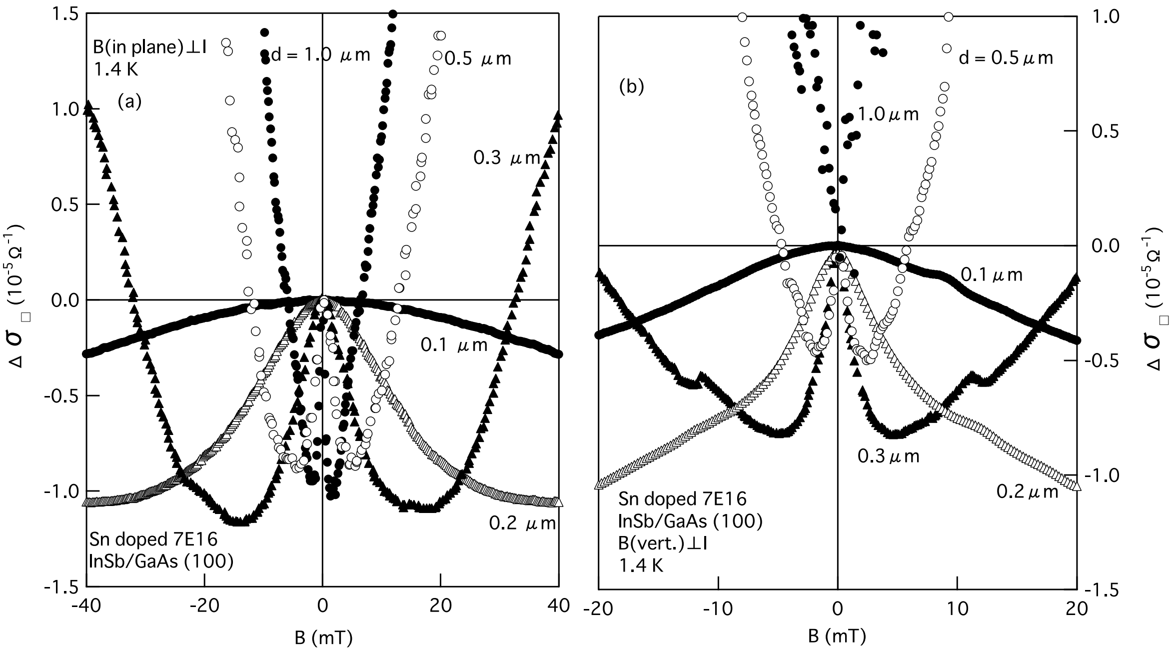

Fig. 3 Transverse magnetoconductance (MC) in extremely weak magnetic fields for five Sn doped films with thickness in the rage 1.0 μm ≧ *d* ≧ 0.1 μm at 1.4 K: (a) parallel MC and (b) perpendicular MC.

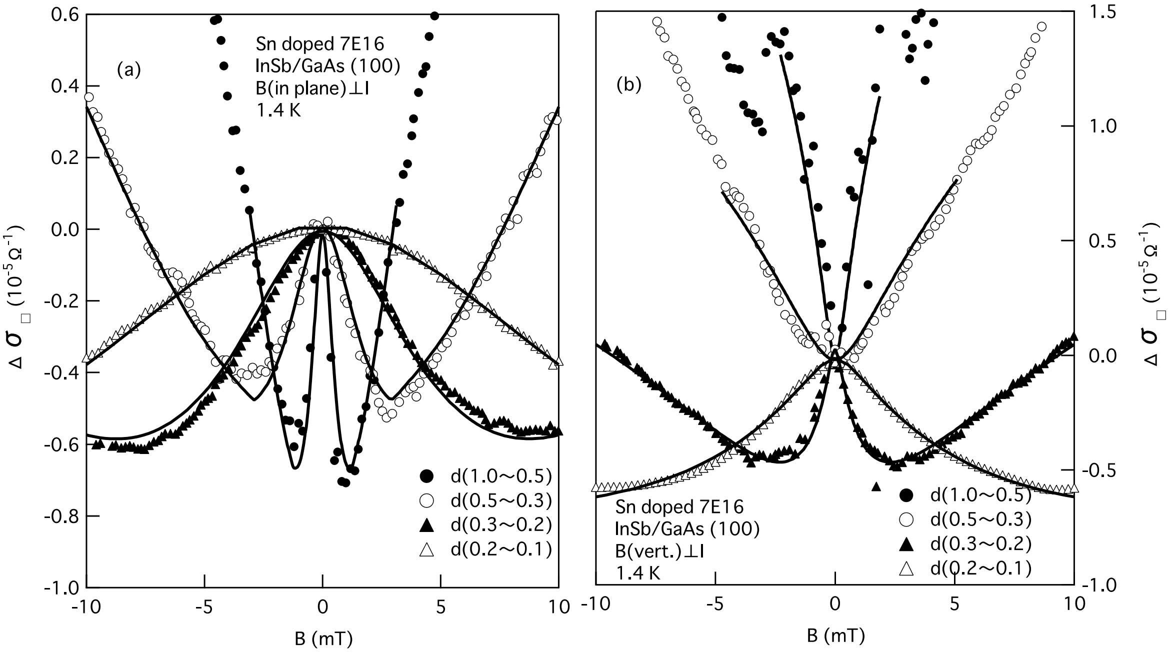

Fig. 4 Variation of transverse MC in extremely weak magnetic fields for four decomposed layers σ(1.0~0.5), σ(0.5~0.3), σ(0.3~0.2) and σ(0.2~0.1) at 1.4 K are fitted: (a) parallel MC and (b) perpendicular MC.